J Appl Biomed
DOI: 10.32725/jab.2022.010
journal homepage: http://jab.zsf.jcu.cz

Journal of Applied Biomedicine

Original research article

Effects of 17-β-estradiol released from shape-memory terpolymer rods on sciatic nerve regeneration after injury and repair with chitosan nerve conduit in female rats

Edyta Olakowska [1 a], Adam Właszczuk [1 a *], Artur Turek [2], Aleksandra Borecka [3], Arkadiusz Liśkiewicz [1], Dariusz Wawro [4], Janusz Kasperczyk [2, 3], Halina Jędrzejowska-Szypułka [1]

[1] *Medical University of Silesia, Faculty of Medical Sciences in Katowice, Department of Physiology, Katowice, Poland*
[2] *Medical University of Silesia, Faculty of Pharmaceutical Sciences in Sosnowiec, Department of Biopharmacy, Sosnowiec, Poland*
[3] *Polish Academy of Sciences, Centre of Polymer and Carbon Materials, Zabrze, Poland*
[4] *Institute of Biopolymers and Chemical Fibres, Łódź, Poland*

Abstract
The aim of this study was to assess 17-β-estradiol (E_2) influence on sciatic nerve regeneration after injury followed by a repair with chitosan conduit in ovariectomized female rats.

The study was performed in 2 groups (n = 16) of rats: OVChit – after excision of a fragment of the sciatic nerve, a chitosan conduit was implanted; OVChitE10 group – additionally to chitosan conduit, shape-memory terpolymer rods based on poly(L-lactide-co-glycolide-co-trimethylene carbonate) releasing 17-β-estradiol for 20 weeks were implanted.

The mean number of regenerating axons and mean fiber area were significantly greater in 17-β-estradiol-treated animals. In this group, the infiltrate of leukocytes was diminished. The presence of 17-β-estradiol receptors alpha and beta in motoneurons in the spinal cord were discovered. This may indicate the location where 17-β-estradiol affects the regeneration of the injured nerve.

Estradiol released from the terpolymer rods for 20 weeks could enhance, to some extent, sciatic nerve regeneration after injury, and diminish the inflammatory reaction. In the future, 17-β-estradiol entrapped in terpolymer rods could be used in the repair of injured peripheral nerves, but there is a need for further studies.

Keywords: 17-β-estradiol (E_2); Chitosan conduit; Inflammation; Sciatic nerve injury; Shape-memory terpolymer

Highlights:
- 17-β-estradiol can enhance sciatic nerve regeneration repaired with chitosan conduit.
- Shape-memory terpolymer allows for prolonged release of estradiol.
- Hormone can diminish infiltration of inflammatory cells in the chitosan conduit.

Introduction

Peripheral nerves can be injured in various traumatic events, such as road accidents, construction works, military operations, and disasters. After peripheral nerve injury, many people suffer from neuropathic pain, loss of motor and sensory function, and poor quality of life (Meyer et al., 2016; Modrak et al., 2020).

Several artificial and natural materials (e.g., collagen, fibrin, polysaccharides) have been used in the management of injured nerves (Alluin et al., 2009; Kalbermatten et al., 2009; Modrak et al., 2020).

One of the promising materials is chitosan (a copolymer of D-glucosamine and N-acetyl-D-glucosamine) that is biocompatible, has antibacterial activity, and can be easily shaped into many forms (Bąk et al., 2017; Kou et al., 2021).

Chitosan-based nerve conduits are used in many experiments to repair injured peripheral nerves (Stenberg et al., 2016; Właszczuk et al., 2016; Zhao et al., 2017).

Because peripheral nerves have the ability to regenerate, all factors that may improve this process are essential. 17-β-estradiol (E_2), a steroid hormone, possesses neuroprotective effects in the nervous system that have been well-documented. The mechanism of estrogen signaling can be genomic (modulation of gene expression) or non-genomic (activation of signaling cascades). Classical genomic pathway involves a binding of E_2 with 2 receptors (ERα and ERβ) and then phosphorylation and dimerization of this complex. Modified complex can bind to estrogen-responsive elements (EREs) in the promoter region

* **Corresponding author:** Adam Właszczuk, Medical University of Silesia, Faculty of Medical Sciences in Katowice, Department of Physiology, Medyków 18, 40-752 Katowice, Poland; e-mail: awlaszczuk@sum.edu.pl
http://doi.org/10.32725/jab.2022.010
[a] These two authors contributed equally to this manuscript.

Submitted: 2021-07-23 • Accepted: 2022-07-07 • Prepublished online: 2022-09-27
J Appl Biomed 20/3: 87–97 • EISSN 1214-0287 • ISSN 1214-021X

of target genes and regulate their transcription (Kövesdi et al., 2021).

Non-genomic signaling pathway begins with the binding of E_2 with membrane receptor GPER1 (G protein-coupled estrogen receptor 1) and certain variants of ERα and ERβ that are able to modulate the activity of extracellular signal-regulated kinases (ERKs)-MAPK (mitogen-activated protein kinase) and PI3K/AKT/mTOR signaling pathway. PI3K/AKT/mTOR signaling pathway is activated in Schwann cells and promotes the remyelination of a nerve (Chen et al., 2016).

E_2 can also promote neuroprotection by indirect regulation of signaling of other receptors, such as IGF1R (insulin growth factor receptor 1), BDNF (brain-derived neurotrophic factor), TGFβ (transforming growth factor beta) or Notch and initiate phosphorylation of CREB (cAMP-responsive element binding protein) which regulate the activity of various neurotrophic factors (Arevalo et al., 2014; Azcoitia et al., 2019; Vrtačnik et al., 2014).

E_2 can probably regulate expression of the same gene through various pathways – genomic and non-genomic (Vrtačnik et al., 2014).

Such influence on the transcription of specific genes may enhance nerve survival, suppress apoptosis, and affect the neuronal structure (Chen et al., 2016; Engler-Chiurazzi et al., 2016, 2017; Siddiqui et al., 2016).

Additionally, E_2 has anti-inflammatory activity in many tissues, probably through the modification of transcription of pro-inflammatory genes, e.g., IL-1β, IL-6, IL-8, IL-12, TNFα (tumor necrosis factor alpha) and MCP-1(chemokine monocyte chemotactic protein 1) (Cox et al., 2015; Herzog et al., 2017; Samantaray et al., 2016).

All substances that can promote nerve recovery can be delivered by the application of implantable, biodegradable formulations based on aliphatic polyesters and polyestercarbonates (Turek et al., 2016, 2018, 2020; Wilińska et al., 2019).

The aim of the present study was to evaluate the influence of E_2 released from the P(L-LA:GA:TMC) shape-memory rods on the regeneration of a sciatic nerve after injury followed by a repair with chitosan nerve conduit in ovariectomized female rats.

Materials and methods

All procedures used in the experiment were performed in accordance with the EU Directive 2010/63/EU for animal experiments and were approved by the Local Ethics Committee for Experiments on Animals in Katowice, Poland (No. 10/2015). Attempts were made to minimize the suffering of rats and to reduce the number of animals used in the study. All animals (the Center for Experimental Medicine of the Medical University of Silesia in Katowice, Poland) were kept in separate cages with a controlled temperature of 25 °C ± 2 °C with a 12-hour light/dark cycle, and free access to water and standard rat chow.

Sixteen ovariectomized adult female Wistar C rats (3 months old, weighing 200–230 g) were randomly divided into 2 groups (n = 8 in each group): OVChit – 7 mm fragment of the sciatic nerve was removed, a conduit with poly(D,L-lactide-co-glycolide) (D,L-PLGA) (75:25) (Resomer 755S, 769797, Sigma-Aldrich, USA) sleeve and chitosan fibers was implanted, OVChitE10 – procedure as above with implantation of terpolymer rods with E_2. The observation period was 20 weeks. All surgical procedures were performed under strict aseptic conditions.

We analyzed the morphology and biodegradation properties of newly synthetized terpolymer rods, the intensity of autotomy behavior in animals, inflammatory reaction in the conduit, E_2 levels in the blood, muscle mass difference, axon morphometry, E_2 receptors alpha (ERα), and beta (ERβ) expression in the spinal cord.

Design of E_2-loaded terpolymer rods

P(L-LA:GA:TMC) with a molar ratio of 55:18:27 (59000 Da) and an average length of lactidyl (l_{LL} – average length of lactidyl blocks), glycolidyl (l_{GG} – average length of glycolidyl blocks) and carbonate (l_{TMC} – average length of carbonate blocks) of 3.6, 1.1, and 1.5, respectively, was synthesized with the use of a low-toxic initiator Zr $(Acac)_4$ (338001, Sigma-Aldrich, USA) at the Centre of Polymer and Carbon Materials of the Polish Academy of Sciences in Zabrze, according to a previously developed methodology (Dobrzyński et al., 2013).

P(L-LA:GA:TMC) was used to prepare rods containing 10% w/w of E_2 (E1024, Sigma-Aldrich, USA) by the hot melt extrusion method. Before the process, raw terpolymer was air-dried and subjected to grinding at a temperature of –196 °C in a cryogenic mill (6870 SPEX, USA). Then E_2 was introduced to the milled terpolymer material. The mixture was vortexed and subsequently placed in a vacuum oven for 14 days with a temperature of 23 °C and a pressure of 80 mBa. The mixture of P(L-LA:GA:TMC) and E_2 was fed to an extruder cylinder heated to 105 °C. This process was carried out in a co-rotating twin screw extruder (Minilab, Thermo-Haake, GE) using a plasticizing screw rotational speed of 20 rpm. The final product was a rod of 1.5 mm in diameter and 10 mm in length (Turek et al., 2016, 2018).

Sterilization of the rods was performed using an electron beam accelerator (absorbed dose 25 kGy) at the Institute of Nuclear Chemistry and Technology of the Center for Radiation Research and Technology – Certificate No. 457/2014/E (Wilińska et al., 2019).

Biodegradation study

The biodegradation study was performed for both the native rods and the rods explanted after experiment. The composition and chain microstructure study of P(L-LA:GA:TMC)-E_2 samples were determined by nuclear magnetic resonance spectroscopy (NMR). Spectra were recorded using a Bruker-Avance II Ultrashield Plus spectrometer operating at 600 MHz (^{1}H) and 150 MHz (^{13}C) using DMSO-d6 as a solvent, with a 5-mm sample tube. ^{1}H NMR spectra were obtained with 32 scans, 11 μs pulse width and 2.65 s acquisition time. ^{13}C NMR spectra were obtained with 20,000 scans, 9.4 μs pulse width and 0.9 s acquisition time. Signals observed in ^{1}H and ^{13}C NMR spectra were assigned to the appropriate sequences in the terpolymer chain, according to the previously described procedure (Turek et al., 2018). The molar percentage of the monomer units of lactide (F_{LL}), glycolide (F_{GG} – molar percentage of glycolidyl units), and carbonate (F_{TMC} – molar percentage of carbonate units) as well as l_{LL}, l_{GG} and l_{TMC} in the terpolymer chain calculations have been previously described (Gębarowska et al., 2011).

Thermal analysis of P(L-LA:GA:TMC)-E_2 was carried out using the differential scanning calorimetry (DSC) method. The TA DSC 2010 apparatus (TA Instruments, New Castle, DE) was used during the measurement. The instrument was calibrated with high-purity indium and gallium and worked under a nitrogen atmosphere (flow rate 50 ml/min).

The terpolymer material was heated at a rate of 20 °C/min. During the first run, the rod samples were heated to 200 °C,

then the melted samples were rapidly cooled to –20 °C. In the second run, the rods were heated within a range of –20 °C to 180 °C. The glass transition temperature (T_g) was determined as the midpoint of the heat capacity change of the amorphous sample, from the second heating run.

M_n and molecular weight distribution (D) of the samples were determined by gel permeation chromatography (GPC) using a Viscotek Rimax chromatograph with two Viscotek 3580 columns and a Shodex SE 61 detector. The process was carried out with chloroform as a solvent with a flow rate of 1 ml/min. The molecular weights were calibrated with polystyrene standards.

Electron micrographs were obtained using a scanning electron microscope (SEM) (Quanta 250 FEG, FEI Company, USA) operating with an acceleration voltage of 5 kV under low vacuum conditions (80 Pa) from secondary electrons collected by a Large Field Detector. The samples were mounted on microscope stubs with the use of double-sided adhesive carbon tape.

Ovariectomy procedure

The rats were anesthetized with a combination of ketamine (80 mg/kg) and xylazine (10 mg/kg) (both compounds POLFA, Poland) intraperitoneally. In the surgical area, the fur on the rat's back was removed and the skin was cleaned with 70% ethanol solution (106577, Amara, Poland). After a midline dorsal skin incision, 2 cm long, inferior to the rib cage and reaching the peritoneal cavity, the adipose tissue was pulled away until the right uterine tube and the ovary was identified. Then, the right ovary with a surrounding fat was gently retracted. After ligation of the distal uterine horn with absorbable 4/0 Vicryl Ethicon (Johnson & Johnson, USA) the right ovary was removed. Afterwards, the uterine horn was returned to the peritoneal cavity, and the peritoneum as well as the muscle layers were sutured with 4/0 Prolene Ethicon (Johnson & Johnson, USA). The skin was sutured with 3/0 Vicryl Ethicon (Johnson & Johnson, USA), and 10% povidone-iodine solution (Teva Pharmaceuticals, Poland) was applied to the surgery area. The left ovary was removed in the same way as described above. The surgery was performed using aseptic techniques. To avoid dehydration, all rats were subcutaneously injected with 2 ml 0.9% sodium chloride (Polpharma, Poland) solution. To prevent pain, 400 mg of paracetamol (suspension 125 mg/5 ml; POLFA, Poland) was applied (200 mg/kg body weight daily).

Nerve conduit preparation

The core of the nerve conduit used for implantation contained 900 chitosan (Primex, Iceland) fibers (multifilament yarn), prepared from medical grade chitosan by means of forming fibers from solution (average molecular polymer mass Mv = 338 kDa, deacetylation degree DD = 82%). The surrounding sleeve was made of D,L-PLGA (Resomer 755S; 769797, Sigma-Aldrich, USA). The chitosan conduit core was 7 mm long with a diameter of 2 mm and surrounded with an 11 mm long sleeve. The sleeve allowed us to obtain 2 mm long cuffs on both sides to cover the proximal and distal nerve stumps. D,L-PLGA sleeve was 40 μm thick. All conduits were sterilized using UV radiation.

Nerve conduit implantation procedure

Two weeks after ovariectomy, all rats were anesthetized by intraperitoneal administration of ketamine 80 mg/kg and xylazine (10 mg/kg-both compounds POLFA, Poland). After disinfection, the skin was cut, the muscles were retracted and the right sciatic nerve was exposed. A single suture (10/0 Vicryl Ethicon (Johnson & Johnson, USA) was passed through the epineurium on each side of the nerve. After that, a 7 mm long fragment of the nerve was cut and removed. Proximal and distal stumps of the nerve were inserted into the sleeve to get in contact with the chitosan conduit core. The epineurium was sutured to the conduit sleeve. The 0.9% sodium chloride (Polpharma, Poland) solution was injected into the core of the conduit. The procedures described above were performed using a stereomicroscope. The muscles and skin were sutured with 4/0 Vicryl Ethicon (Johnson & Johnson, USA).

Blood samples collection

Blood samples were collected from the orbital plexus in all animals before ovariectomy, 2 weeks after ovariectomy and before euthanasia. E_2 levels were estimated by standard kit according to the manufacturer's instruction (mouse/rat Estradiol ELISA Kit, ES180S-100, Calbiotech, USA). All samples were analyzed in a single assay.

Assessment of autotomy

The intensity of autotomy (spontaneous biting of the fingers of a denervated limb caused by pain) was scored using Wall scale 20 weeks after surgery: for complete amputation of 0–2 claws the point score was 0, more than 2 claws-1 point, distal and proximal phalanx-1 point for each finger, metatarsus-1 point, and tarsus-1 point (Wall et al., 1979).

Muscle mass measurement

Twenty weeks after the surgery, all rats were euthanized with 100 mg/kg ketamine and 10 mg/kg xylazine intraperitoneally (both compounds POLFA, Poland). The muscles of both hind limbs were dissected carefully from the surrounding tissues, and while still wet, weighed on a digital laboratory scale.

Histological and immunohistochemical analysis

Both sciatic nerves with chitosan conduit (right hind limb) and from the intact side (left hind limb) were excised and preserved in 4% formaldehyde solution (114321734, Chempur, Poland) in PBS (phosphate buffered saline) (524650, Calbiochem, USA) for 12 hours and then dehydrated in 10% of sucrose solution (117720907, Chempur, Poland), embedded in TissueTek (Sakura, Japan) optimum cutting temperature freezing media and deeply frozen. All specimens were cut into 10-μm-thick sections longitudinally using a cryotome, and placed on microscopic slides. Nerve sections were stained with the Masson Trichrome method. Slides were photographed using the Zeiss AxioCam ICm1 camera mounted on the Zeiss Axio Scope A1 microscope. Inflammatory cells were counted using ImageJ software.

Spinal cord

After skin incision and muscle dissection, laminectomy was carried out and segments L4–L6 were removed. Spinal cord fragments were kept for 24 hours in 20% of sucrose with PBS at 4 °C and then embedded in TissueTek (Sakura, Japan). After this, sagittal sections (20 μm) were obtained from samples by means of cryotome (Leica, Germany), mounted on SuperFrost+ slides (Menzel Glaeser, Germany) and used for immunohistochemical analysis. Immunohistochemistry with the following antibodies: anti-ER α (ERα-10 μg/ml, PAB050R001, Cloud-Clone Corp., USA) and anti-ER β (ERβ-10 μg/ml, PAA437R001, Cloud-Clone Corp., USA) both labeled with AlexaFluor 488 dye (A-1108, Thermo Fisher Scientific, USA) was performed according to the manufacturer's instruction. Slides were photographed using the Zeiss AxioCam ICm1 camera mounted on the Zeiss Axio Scope A1 microscope.

Morphometric analysis

Twenty weeks after the surgery, all rats were euthanized. Segments of the right sciatic nerves were dissected. Collected nerves were immersed immediately in cold (4 °C) fixative (2.5% of glutaraldehyde solution (23115.01, Serva, Germany) and 0.5% of sucrose solution in 0.1 M cacodylate buffer (20840, 20835), pH 7.4; Sigma-Aldrich, USA). The specimens were kept well distended and oriented for 24 hours, and then, post-fixed in 1.5% of osmium tetroxide solution and embedded in Epon (both Sigma-Aldrich, USA). Intact left sciatic nerves were prepared as above.

Five pictures of each nerve section were acquired using the Zeiss AxioCam ICm 1 camera mounted on the Zeiss Axio Scope A1 microscope. Each picture covered an area of 7904 μm^2 (1388 × 1038 pixels) of the nerve section. Five pictures per animal were analyzed using ImageJ software to examine the following parameters: mean number of nerve fibers per picture, mean fiber area, and total fiber area.

Statistical analysis

Data in the text were given as mean ± standard deviation (SD). Data in the figures were given as described. Statistical parameters were analyzed with Shapiro–Wilk test, *T*-test, Mann–Whitney test, two-way RM ANOVA and Sidak's *post hoc* test using Graph Pad Prism 8 software. Statistical significance was accepted at $p < 0.05$. Significance is marked: $p < 0.05$ (*), $p < 0.01$ (**), $p < 0.001$ (***).

Results

Biodegradation study

The analysis of ^{1}H NMR spectra did not reveal the significant changes in the monomer unit distribution in the P(L-LA:GA:TMC)-E_2 during 140 days of the biodegradation process (Fig. 1A). Initially P(L-LA:GA:TMC) contained ~55 mol % of the F_{LL}, ~18 mol % of the F_{GG} and ~27 mol % of the F_{TMC} units and pointed values remained at the same level (Table 1).

^{13}C NMR spectra revealed no changes in the chain microstructure (l_{LL}, l_{GG} and l_{TMC}) during biodegradation period (Fig. 1B).

DSC curves of the second heating of P(L-LA:GA:TMC)-E_2 revealed noticeable changes in T_g after 140 days of biodegradation (Fig. 2A, Table 1).

The GPC analysis showed a significant decrease of M_n during 140 days of biodegradation, from 45.8 kDa to 0.5 kDa (Table 1). *D* decreased from 2.8 to 2.4 in this period.

The outer and inner morphology of native P(L-LA:GA:TMC)-E_2 rods performed by using the SEM method exhibited a solid surface. Biodegradation in period 140 days did not reveal significant changes in morphology (Fig. 2B).

Autotomy score

Mean autotomy intensity was 1.25 ± 2.12 in OVChit group and 1.57 ± 2.29 in OVChitE10 (according to 25). The difference was not statistically significant (Fig. 3).

Muscle mass measurement

Mean muscle mass difference (left hind limb vs. right hind limb) was 1.88 ± 1.0 g in the OVChit group and 1.60 ± 0.59 g in the OVChitE10 group. The difference between the groups was not statistically significant (Fig. 4).

Number of inflammatory cells

The mean number of leukocytes counted in twenty-five 1/400 mm^2 squares in the core of each conduit was 69.73 ± 16.23 in the OVChit group and 41.39 ± 8.81 in the OVChitE10 group. The difference was statistically significant (**, $p = 0.0012$) (Fig. 5A). Inflammatory cells visible in the conduit are presented in Fig. 5B.

Histology and morphometric findings

Twenty weeks after surgery, newly growing axons were present inside the chitosan conduits and they bridged the site of injury. These new axons were thinner than those in the unaffected nerve, but their number was higher in the groups treated with E_2, and the axons covered a greater area than in non-treated groups.

The mean number of nerve fibers per picture was 69.78 ± 53.41 in the OVChit group and 83.86 ± 39.8 in the OVChitE10 group. The difference was statistically significant (*, $p = 0.0179$) (Fig. 6A). Mean fiber area was 3.25 ± 1.33 μm^2 in the OVChit group and 3.87 ± 1.35 μm^2 in the OVChitE10 group. The difference was statistically significant (*, $p = 0.0246$) (Fig. 6B). Regenerated axons are presented in Fig. 6C.

Total fiber area was 243.4 ± 199.3 μm^2 in the OVChit group, 334.3 ± 220.9 μm^2 in the OVChitE10 group, and 1736 ± 228 μm^2 in the control (intact nerves) group. The difference between the OVChit group and the OVChitE10 group was statistically significant (*, $p = 0.0336$) (Fig.7A). The differences in total fiber area between the intact side and experimental groups were significant (***, $p < 0.0001$) (Fig. 7B).

The presence of estrogen receptors, alpha and beta, in ventral horns of the spinal cord at L4–L6 levels with the use of specific antibodies has been revealed. The results are shown in Fig. 8.

Serum E_2 levels

Serum levels of E_2 in all ovariectomized rats were estimated in 2 different time points. Mean serum E_2 level 14 days after ovariectomy was 11.59 ± 13.52 pg/ml in the OVChit group and 20.03 ± 13.45 pg/ml in the OVChitE10 group. The difference was not statistically significant. Mean serum E_2 level 42 days after ovariectomy was 6.09 ± 10.65 pg/ml in the OVChit group and 89.82 ± 26.27 pg/ml in the OVChitE10 group. The difference was statistically significant (**, $p < 0.0016$) (Fig. 9).

Table 1. Parameters characterizing the P(L-LA:GA:TMC)-E_2 rods after 0 and 140 days of biodegradation

Time (days)	F_{LL}	F_{GG}	F_{TMC}	l_{LL}	l_{GG}	l_{TMC}	T_g	M_n	D
0	55.3	17.7	27.0	3.6	1.1	1.5	34.2	45.8	2.8
140	55.4	17.7	26.9	3.6	1.1	1.5	33.9	0.5	2.4

F_{LL} – molar percentage of lactidyl units; F_{GG} – molar percentage of glycolidyl units; F_{TMC} – molar percentage of carbonate units; l_{LL} – average length of lactidyl blocks; l_{GG} – average length of glycolidyl blocks; l_{TMC} – average length of carbonate blocks; T_g – glass transition temperature (°C); M_n – molecular weight (kDa); D – molecular weight distribution.

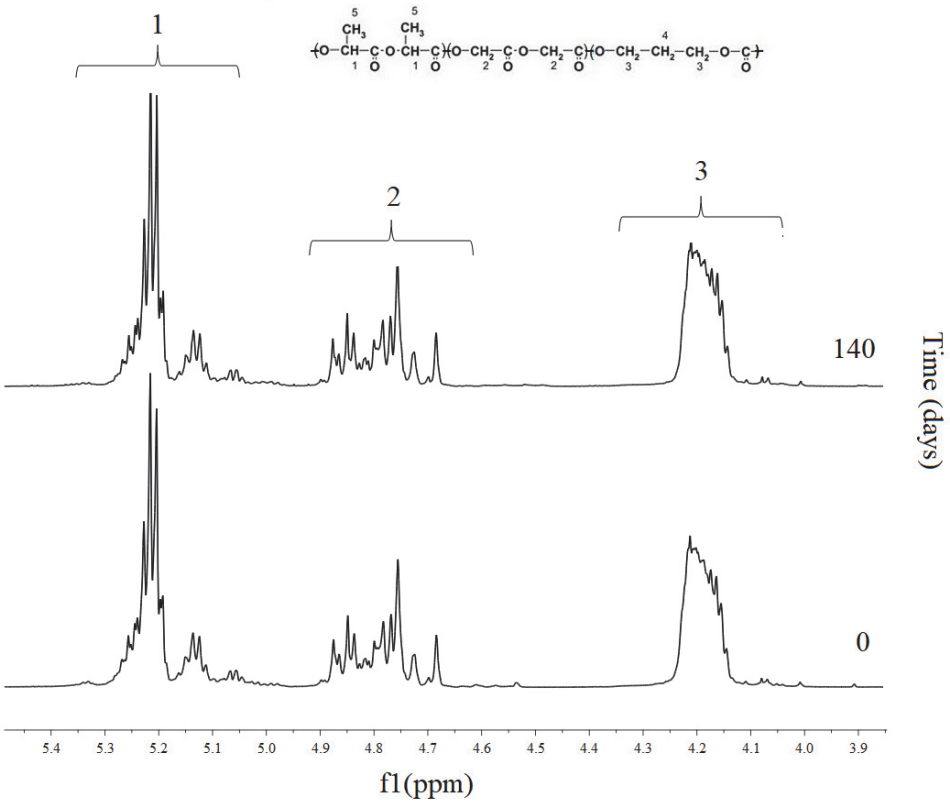

Fig. 1A. ^{1}H NMR spectra (600 MHz, DMSO-d6) of the P(L-LA:GA:TMC)-E_2 rods with during 140 days of biodegradation [methine proton region of the lactidyl units (1) and methylene proton region of the glycolidyl (2) and carbonate units (3)]

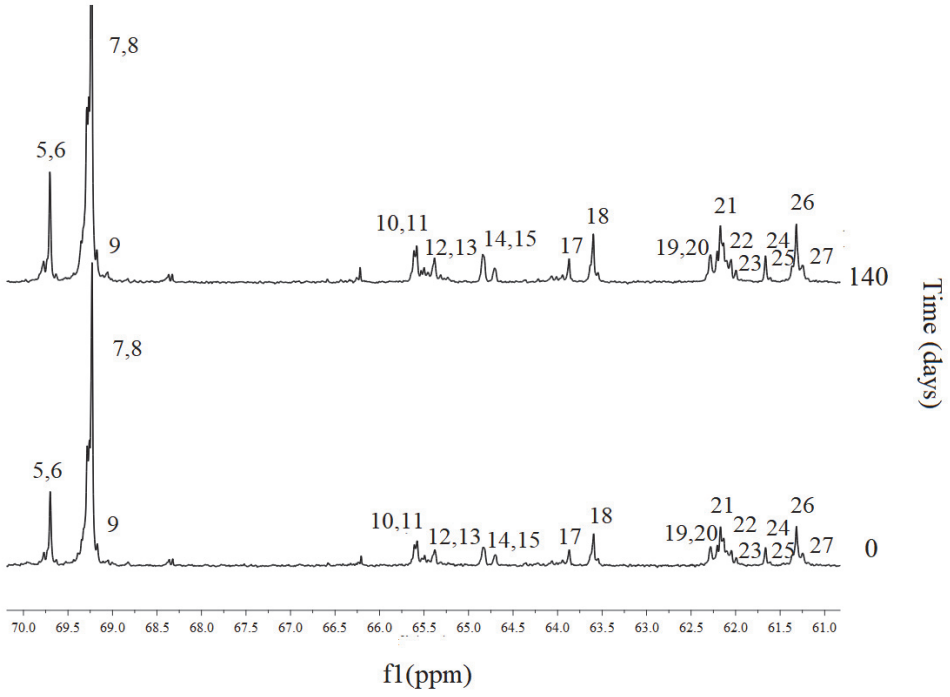

Fig. 1B. ^{13}C NMR (150 MHz, DMSO-d6) of the P(L-LA:GA:TMC)-E_2 rods during 140 days of biodegradation [methine carbon region of the lactidyl units (*LL*) and methylene carbon region of the glycolidyl (*GG*) and carbonate units(T)]. 5-*GLLT* + *GLLLT*, 6-*TLLLL* + *LLLLT*, 7-*LLLL*, 8-*LLGG*, 9-*GLG*, 10-*TT'G* + *GGT'GG* + *TGT'GG*, 11-*GGTT*, 12-*GGT'GT* + *GT'GT*, 13-*GGT'GT* + *TT'L* + *LTT'*, 14-*TT'T* + *TTT'* + *TT"G*, 15-*TT'GG*, 17-*TGT* + *TGGL* + *TGGT*, 18-*LGGGT* + *TGGGT* + *GGGGT*, 19-*TT'L* + *LT"T*, 20-*LT'L* + *LT"L*, 21-*GGT'T*, 22-*GGT"GT* + *GGT"GG*, 23-*TGT"GG* + *TGT'GT*, 24-*TGGGG* + *TGG*, 25-*TGGT*, 26-*GGLL*, 27-*GGGG*.

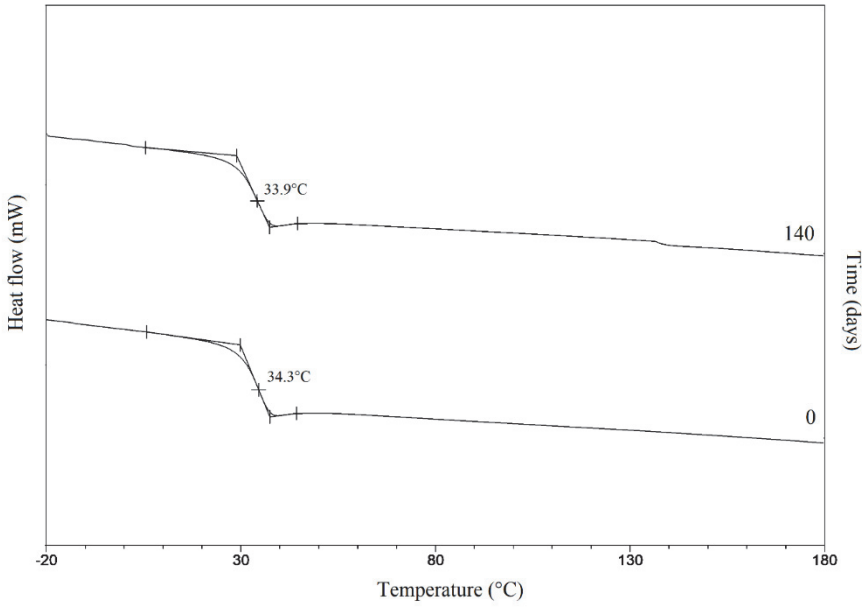

Fig. 2A. DSC curves of the second heating run for E_2-loaded P(L-LA:GA:TMC)-E_2 rods after 0 and 140 days of biodegradation

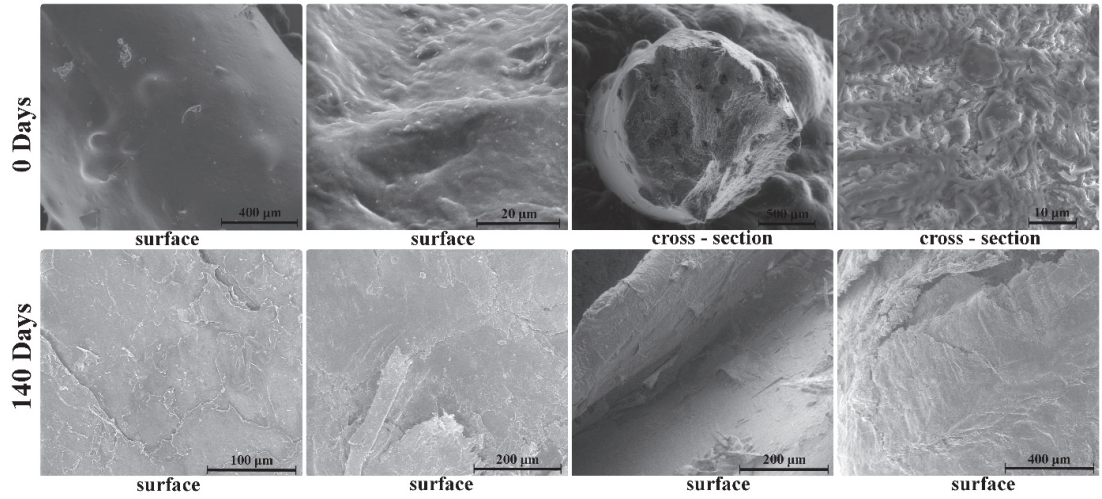

Fig. 2B. SEM images of P(L-LA:GA:TMC)-E_2 rods biodegraded for 0 days and after 140 days

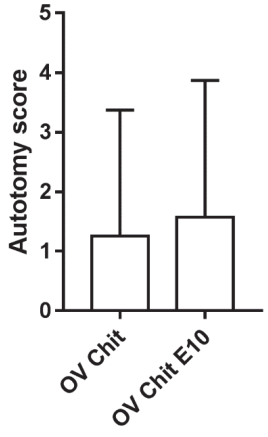

Fig. 3. Autotomy intensity score. All data are presented as the mean + SD.

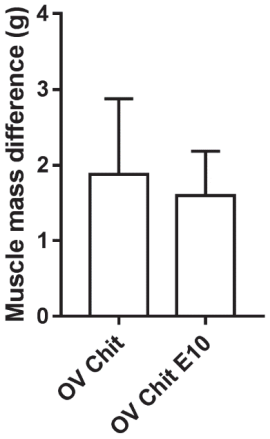

Fig. 4. Muscle mass difference between left and right hind limb. All data are presented as the mean + SD.

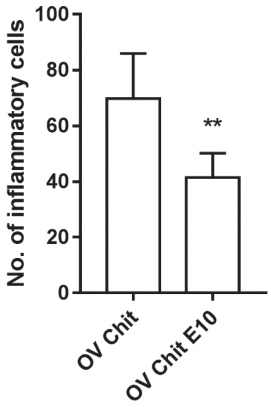

Fig. 5A. The mean number of leukocytes counted in twenty-five 1/400 mm^2 squares in the core of each conduit. All data are presented as the mean + SD. The difference was statistically significant, $p = 0.0012$ (**) (unpaired t-test).

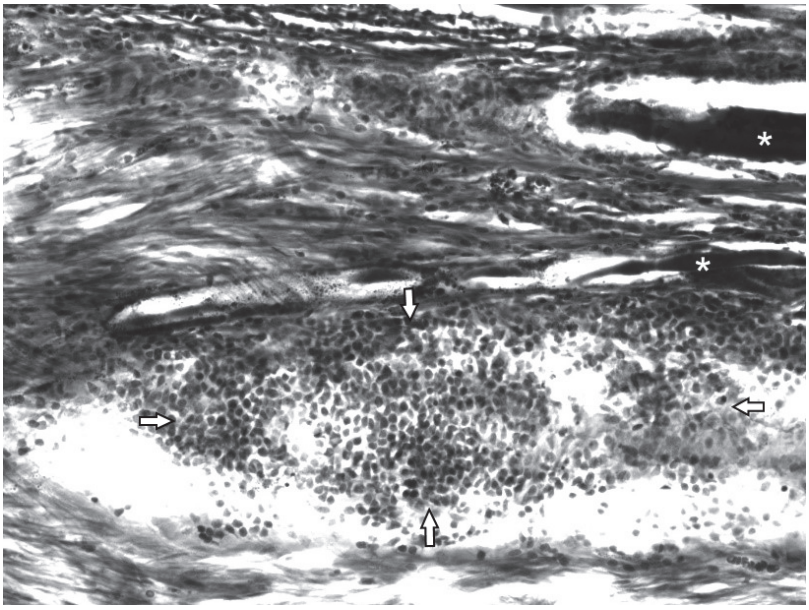

Fig. 5B. Inflammatory cells visible in the chitosan conduit. (* – chitosan fibres, arrows – area with inflammatory cells). Sciatic nerve injury induces leukocyte invasion and infiltration of the nerve and surrounding tissues. Leukocytes can produce various pro-inflammatory chemokines, e.g., TNFα, IL-1β, IL-6, metalloproteinases, ROS (reactive forms of oxygen) which enhance inflammation and decrease the regeneration rate of the lesioned nerve (Nguyen et al., 2007). Additionally, this inflammatory reaction can also be triggered by a chitosan conduit that can induce leukocytes (mainly neutrophils) infiltration at the site of injury (Minami et al., 1998).

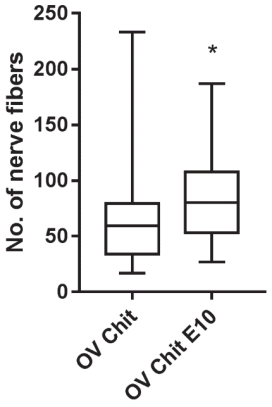

Fig. 6A. Mean number of regenerating nerve fibers. All data are presented as the mean, minimum, maximum, 25% percentile and 75% percentile; $p = 0.0179$ (*) (Mann–Whitney test).

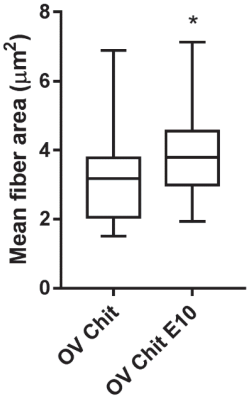

Fig. 6B. Mean fiber area. All data are presented as the mean, minimum, maximum, 25% percentile and 75% percentile; $p = 0.0246$ (*) (Mann–Whitney test).

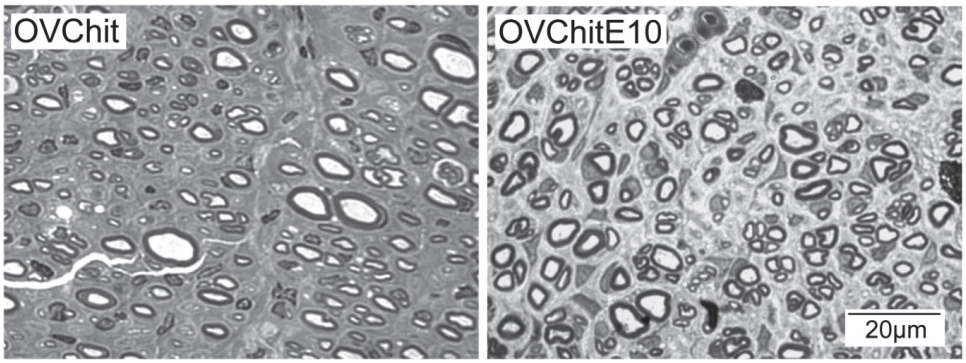

Fig. 6C. Transverse nerve sections showing regenerating axons. Osmium tetroxide staining. Light microscopy, magnification × 1000.

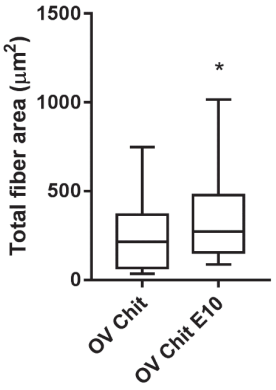

Fig. 7A. Total fiber area. All data are presented as the mean, minimum, maximum, 25% percentile and 75% percentile; $p = 0.0336$ (*) (Mann–Whitney test).

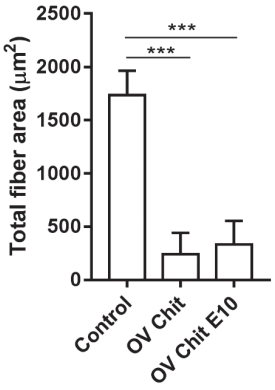

Fig. 7B. Differences between control (intact nerves) and experimental groups in total fiber area. All data are presented as the mean + SD; $p < 0.0001$ (***) (Kruskal–Wallis test).

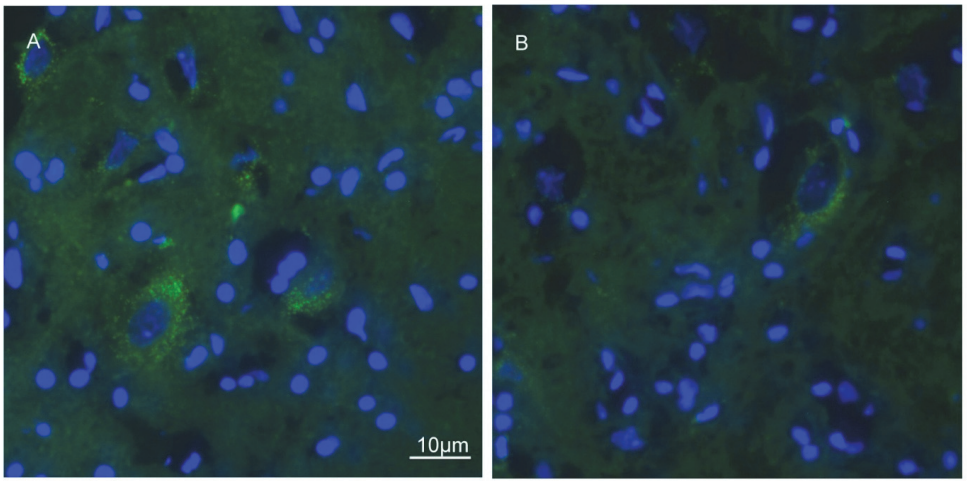

Fig. 8. Estrogen receptors (green): ERα (**A**) and ERβ (**B**) in rat spinal cord neurons (ventral horn, L4). OVChit group, left (intact) side of the body. Cell nuclei shown in blue (DAPI).

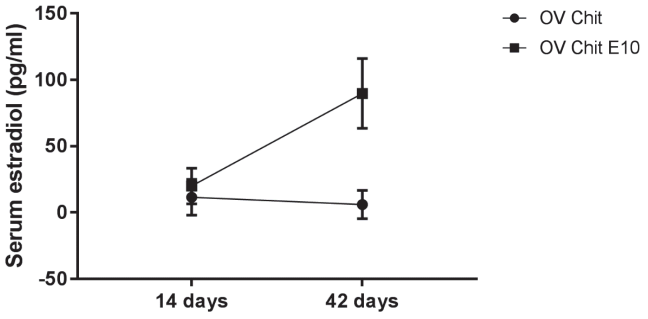

Fig. 9. Serum estradiol levels. All data are presented as the mean ± SD; $p < 0.0016$ (**) (Two-way ANOVA test).

Discussion

Functional recovery of the injured nerve is still a great medical challenge. Currently, the gold standard is an autologous nerve graft, but intensive development of various biomaterials can be a promising alternative. We focused on the repair of the transected sciatic nerves with chitosan conduits supported by prolonged release of E_2 from the newly designed terpolymer rods.

Many authors have revealed the favorable effects of estrogen on the regeneration of neurons *in vitro* and *in vivo* (Caceres et al., 2011; Huppenbauer et al., 2005; Murashov et al., 2004; Smith et al., 2009).

We implanted terpolymer rods releasing E_2 in a prolonged manner that was non-irritating to the surrounding tissues. The rods had a shape-memory property and ensured low invasiveness. Another advantage of terpolymers was its biodegradability and low invasiveness, which allowed us to eliminate the removal of the rods during the experiment. A stable degradation process with prolonged release of E_2 has been confirmed in a previous study (Turek et al., 2016). The biodegradation study of terpolymer rods revealed the same character compared to *in vitro* degradation, similar to other formulations (Turek et al., 2015).

To the authors' knowledge, the effects of prolonged release of E_2 from such terpolymer rods or other implanted formulations on nerve regeneration is yet to be studied *in vivo*.

The study was performed on female ovariectomized rats, enabling the control of serum concentrations of released E_2, and creating a situation observed in menopausal women with E_2 supplementation.

Morphometric analysis after 20 weeks revealed significant differences in nerve regeneration between the groups. In E_2-treated animals the mean number of regenerating nerve fibers and mean fiber area were higher compared to the non-treated group.

A possible influence of E_2 on the regeneration of the peripheral nerve injury was only examined in a few experiments.

In our study, some morphometric parameters were similar to those examined by Islamov et al. (2002). They examined the influence of E_2 on the regeneration of the crushed sciatic nerve in ovariectomized female mice, revealing a significantly greater total number of regenerating nerve fibers at 1 week after injury and increased mean axonal area 2 weeks after crush in E_2 group. The authors estimated a total number of regenerating axons, but we counted a mean number of regenerating nerve fibers, so these parameters cannot be compared. They observed enhanced functional recovery, growth, and maturation of regenerating nerve fibers in E_2-treated mice, which may suggest promotion of regeneration of injured sciatic nerve by E_2. In our experiment, there was a statistically significant difference in the total fiber area between E_2-treated and non-treated rats.

We discovered the presence of E_2 receptors α and β in motor neurons located in the segments L4–L6 of spinal cord, but we did not count them. This could be one of the locations where E_2 affects the sciatic nerve regeneration. Other authors also confirm the presence of estrogen receptors in the spinal cord after E_2 treatment (Samantaray et al., 2016; Sribnick et al., 2006).

We observed an inflammatory infiltration consisting of leukocytes (mostly lymphocytes) in the chitosan conduit. In the E_2-treated group, this inflammatory reaction was decreased in comparison to the non-treated one. We do not know if diminished infiltration of inflammatory cells in the OVChitE10 group was caused by chitosan fragments or anti-inflammatory action of E_2. Hsu et al. (2013) observed that chitosan fragments induced inflammatory cells infiltration near to the conduit. It could be associated with the interaction with specific toll-like receptors on the immune cell surface, and this infiltration can affect regeneration of the nerve fibers and recovery.

Anti-inflammatory activity of E_2 has been revealed in various studies (Herzog et al., 2017; Samantaray et al., 2016; Vegeto et al., 2002). Santizo et al. (2000) suggested, that decreased leukocyte infiltration may be an important mechanism in estrogen-mediated neuroprotection.

Nobakhti-Asfhar et al. (2016) conducted an experiment on the sciatic nerve transection model in female ovariectomized rats with silicone conduit repair and E_2 supplementation. E_2-treated rats had significantly greater nerve fibers, axon diameter, myelin sheath thickness, biomechanical parameters, improved locomotor function, and nerve conduction velocity, in comparison with the E_2-non-treated group. Gastrocnemius muscle weight was significantly greater in the E_2-treated group. The authors revealed that local administration of E_2 in the silicone conduit resulted in faster functional recovery of the injured nerve and better muscle reinnervation.

In our study, the gastrocnemius muscle mass was also assessed, but we did not observe significant differences between groups.

A limitation may be that we cannot exactly compare our results with other studies due to a limited number of articles concerning the influence of E_2 on peripheral nerve regeneration in ovariectomized female rats.

Conclusions

E_2 released from the terpolymer rod in a prolonged manner for many weeks could enhance, to some extent, sciatic nerve regeneration after injury, and diminish the inflammatory reaction. In the future, E_2 coupled with biopolymer rods could possibly be used in the repair of injured peripheral nerves.

Funding
This study was supported by grant PCN-1-090/K/0/O (Medical University of Silesia, Katowice, Poland).

Ethical aspects and conflict of interests
The authors have no conflict of interests to declare.

References

Alluin O, Wittmann C, Marqueste T, Chabas J-F, Garcia S, Lavaut M-N, et al. (2009). Functional recovery after peripheral nerve injury and implantation of a collagen guide. Biomaterials 30(3): 363–373. DOI: 10.1016/j.biomaterials.2008.09.043.

Arevalo M-A, Azcoitia I, Garcia-Segura LM (2014). The neuroprotective actions of oestradiol and oestrogen receptors. Nat Rev Neurosci 16(1): 17–29. DOI: 10.1038/nrn3856.

Azcoitia I, Barreto GE, Garcia-Segura LM (2019). Molecular mechanisms and cellular events involved in the neuroprotective actions of estradiol. Analysis of sex differences. Front Neuroendocrinol 55, 100787. DOI: 10.1016/j.yfrne.2019.100787.

Bąk M, Gutkowska ON, Wagner E, Gosk J (2017). The role of chitin and chitosan in peripheral nerve reconstruction. Polim Med 47(1): 43–47. DOI: 10.17219/pim/75653.

Caceres LG, Uran SL, Zorilla Zubilete MA, Romero JI, Capani F, Guelman LR (2011). An early treatment with 17-beta estradiol is neuroprotective against the long-term effects of neonatal ionizing radiation exposure. J Neurochem 118(4): 626–635. DOI: 10.1111/j.1471-4159.2011.07334.x.

Chen Y, Guo W, Xu L, Li W, Cheng M, Hu Y, Xu W (2016). 17β-Estradiol Promotes Schwann Cell Proliferation and Differentiation, Accelerating Early Remyelination in a Mouse Peripheral Nerve Injury Model. Biomed Res Int 2016: 7891202. DOI: 10.1155/2016/7891202.

Cox A, Varma A, Barry J, Vertegel A, Banik N (2015). Nanoparticle Estrogen in Rat Spinal Cord Injury Elicits Rapid Anti-Inflammatory Effects in Plasma, Cerebrospinal Fluid, and Tissue. J Neurotrauma 32(18): 1413–1421. DOI: 10.1089/neu.2014.3730.

Dobrzyński P, Kasperczyk J, Smola A, Pastusiak M, Sobota M, Jaworska J (2013). Bioresorbable and biocompatible thermoplastic elastomer having a shape memory, particularly for biomedical applications and a process for their preparation. EP 2647656 A2.

Engler-Chiurazzi EB, Brown CM, Povroznik JM, Simpkins JW (2017). Estrogens as neuroprotectants: Estrogenic actions in the context of cognitive aging and brain injury. Prog Neurobiol 157: 188–211. DOI: 10.1016/j.pneurobio.2015.12.008.

Engler-Chiurazzi EB, Singh M, Simpkins JW (2016). From the 90's to now: A brief historical perspective on more than two decades of estrogen neuroprotection. Brain Res 1633: 96–100. DOI: 10.1016/j.brainres.2015.12.044.

Gębarowska K, Kasperczyk J, Dobrzynski P, Scandola M, Zini E, Li S (2011). NMR analysis of the chain microstructure of biodegradable terpolymers with shape memory properties. Eur Polym J 47(6): 1315–1327. DOI: 10.1016/j.eurpolymj.2011.02.022.

Herzog R, Zendedel A, Lammerding L, Beyer C, Slowik A (2017). Impact of 17beta-estradiol and progesterone on inflammatory and apoptotic microRNA expression after ischemia in rat model. J Steroid Biochem Mol Biol 167: 126–134. DOI: 10.1016/j.jsbmb.2016.11.018.

Hsu S-H, Kuo W-C, Chen Y-T, Yen C-T, Chen Y-F, Chen K-S, et al. (2013). New nerve regeneration strategy combining laminin-coated chitosan conduits and stem cell therapy. Acta Biomater 9(5): 6606–6615. DOI: 10.1016/j.actbio.2013.01.025.

Huppenbauer CB, Tanzer L, DonCarlos LL, Jones KJ (2005). Gonadal steroids attenuation of developing hamster facial motoneuron loss by axotomy: equal efficacy of testosterone, dihydrotestosterone and 17-beta estradiol. J Neurosci 25(16): 4004–4013. DOI: 10.1523/JNEUROSCI.5279-04.2005.

Islamov RR, Hendricks WA, Jones RJ, Lyall GJ, Spanier NS, Murashov AK (2002). 17beta-estradiol stimulates regeneration of sciatic nerve in female mice. Brain Res 943(2): 283–286. DOI: 10.1016/s0006-8993(02)02827-5.

Kalbermatten DF, Pettersson J, Kingham PJ, Pierer G, Wiberg M, Terenghi G (2009). New fibrin conduit for peripheral nerve repair. J Reconstr Microsurg 25(1): 27–33. DOI: 10.1055/s-0028-1090619.

Kou SG, Peters LM, Mucalo MR (2021). Chitosan: A review of sources and preparation methods. Int J Biol Macromol 169: 85–94. DOI: 10.1016/j.ijbiomac.2020.12.005.

Kövesdi E, Szabó-Meleg E, Abrahám IM (2021). The role of estradiol in traumatic brain injury: mechanism of treatment potential. Int J Mol Sci 22(1): 11. DOI: 10.3390/ijms22010011.

Meyer C, Stenberg L, Gonzales-Perez F, Wrobel S, Ronchi G, Udina E, et al. (2016). Chitosan-film enhanced chitosan nerve guides for long- distance regeneration of peripheral nerves. Biomaterials 76: 33–51. DOI: 10.1016/j.biomaterials.2015.10.040.

Minami S, Suzuki H, Okamoto Y, Fujinaga T, Shigemasa Y (1998). Chitin and chitosan activate complement via the alternative pathway. Carbohydr Polym 36(2–3): 151–155. DOI: 10.1016/S0144-8617(98)00015-0.

Modrak M, Talukder MAH, Gurgenashvili K, Noble M, Elfar JC (2020). Peripheral nerve injury and myelination: Potential therapeutic strategies. J Neurosci Res 98(5): 780–795. DOI: 10.1002/jnr.24538.

Murashov AK, Islamov RR, McMurray RJ, Pak ES, Weidner DA (2004). Estrogen increases retrograde labeling of motoneurons: evidence of a nongenomic mechanism. Am J Physiol Cell Physiol 287(2): C320–326. DOI: 10.1152/ajpcell.00542.2003.

Nguyen HX, O'Barr TJ, Anderson AJ (2007). Polymorphonuclear leukocytes promote neurotoxicity through release of matrix metalloproteinases, reactive oxygen species, and TNF-alpha. J Neurochem 102(3): 900–912. DOI: 10.1111/j.1471-4159.2007.04643.x

Nobakhti-Asfhar A, Najafpour A, Mohammadi R, Zarei L (2016) Assessment of neuroprotective effects on local administration of 17-beta-estradiol on peripheral nerve regeneration in ovariectomized female rats. Bull Emerg Trauma 4(3): 141–149.

Samantaray S, Das A, Matzelle DC, Yu SP, Wei L, Varma A, et al. (2016). Administration of low dose estrogen attenuates persistent inflammation, promotes angiogenesis and improves locomotor function following chronic spinal cord injury. J Neurochem 137(4): 604–617. DOI: 10.1111/jnc.13610.

Santizo RA, Anderson S, Ye S, Koenig HM, Pelligrino DA (2000). Effects of estrogen on leukocyte adhesion after transient forebrain ischemia. Stroke 31(9): 2231–2235. DOI: 10.1161/01.str.31.9.2231.

Siddiqui AN, Siddiqui N, Khan RA, Kalam A, Jabir NR, Kamal MA, et al. (2016). Neuroprotective role of steroidal sex hormones: an overview. CNS Neurosci Ther 22(5): 342–350. DOI: 10.1111/cns.12538.

Smith PG, George M, Bradshaw S (2009). Estrogen promotes sympathetic nerve regeneration in rat proximal urethre. Urology 73(6): 1392–1396. DOI: 10.1016/j.urology.2008.11.052.

Sribnick EA, Matzelle DD, Ray SK, Banik NL (2006). Estrogen treatment of spinal cord injury attenuates calpain activation and apoptosis. J Neurosci Res 84(5): 1064–1075. DOI: 10.1002/jnr.21016.

Stenberg L, Kodama A, Lindwall-Blom C, Dahlin LB (2016). Nerve regeneration in chitosan conduits and in autologous nerve grafts in healthy and in type 2 diabetic Goto-Kakizaki rats. Eur J Neurosci 43(3): 463–473. DOI: 10.1111/ejn.13068.

Turek A, Borecka A, Janeczek H, Sobota M, Kasperczyk J (2018). Formulation of delivery systems with risperidone based on biodegradable terpolymers. Int J Pharm 548(1): 159–172. DOI: 10.1016/j.ijpharm.2018.06.051.

Turek A, Kasperczyk J, Jelonek K, Borecka A, Janeczek H, Libera M, et al. (2015). Thermal properties and morphology changes in degradation process of poly(L-lactide-co-glycolide) matrices with risperidone. Acta Bioeng Biomech 17(1): 11–20.

Turek A, Olakowska E, Borecka A, Janeczek H, Sobota M, Jaworska J, et al. (2016). Shape-memory terpolymer rods with 17-β-estradiol for the treatment of neurodegenerative diseases: *in vitro* and *in vivo* study. Pharm Res 33(12): 2967–2978. DOI: 10.1007/s11095-016-2019-9.

Turek A, Stoklosa K, Borecka A, Paul-Samojedny M, Kaczmarczyk B, Marcinkowski A, Kasperczyk J (2020). Designing biodegradable wafers based on poly(L-lactide-co-glycolide) and poly(glycolide-co-ε-caprolactone) for the prolonged and local release of idarubicin for the therapy of glioblastoma multiforme. Pharm Res 37(5): 90. DOI: 10.1007/s11095-020-02810-2.

Vegeto E, Ciana P, Maggi A (2002). Estrogen and inflammation: hormone generous action spreads to the brain. Mol Psychiatry 7(3): 236–238. DOI: 10.1038/sj.mp.4001007.

Vrtačnik P, Ostanek B, Mencej-Bedrač S, Marc J (2014). The many faces of estrogen signaling. Biochem Med 24(3): 329–342. DOI: 10.11613/BM.2014.035.

Wall PD, Devor M, Inbal R, Scadding JW, Schonfeld D, Seltzer Z, Tomkiewitz MM (1979). Autotomy following peripheral nerve lesions: experimental anaesthesia dolorosa. Pain 7(2): 103–111. DOI: 10.1016/0304-3959(79)90002-2.

Wilińska J, Turek A, Borecka A, Rech J, Kasperczyk J (2019). Electron beam sterilization of implantable rods with risperidone and with 17-β-estradiol: a structural, thermal and morphology study. Acta Bioeng Biomech 21(3): 39–47. DOI: 10.5277/ABB-01399-2019-01.

Wlaszczuk A, Marcol W, Kucharska M, Wawro D, Palen P, Lewin-Kowalik J (2016). Poly (D, L-Lactide-Co-Glycolide) tubes with multifilament chitosan yarn or chitosan sponge core in nerve regeneration. J Oral Maxillofac Surg 74(11): 2327.e1–2327.e12. DOI: 10.1016/j.joms.2016.07.009.

Zhao Y, Wang Y, Gong J, Yang L, Niu C, Ni X, et al. (2017). Chitosan degradation products facilitate peripheral nerve regeneration by improving macrophage-constructed microenvironments. Biomaterials 134: 64–77. DOI: 10.1016/j.biomaterials.2017.02.026.